Master of Science in Electrical Engineering with
Emphasis Telecommunication Systems
September 2021

Towards Underwater UV Communication- Simulation and Experimentation on Penetration of UV Radiation into Sea water.

Subhash Chandra Ranga

Faculty of Engineering, Blekinge Institute of Technology, 371 79 Karlskrona, Sweden

This thesis is submitted to the Faculty of Engineering at Blekinge Institute of Technology in partial fulfilment of the requirements for the degree of Master of Science in Electrical Engineering with Emphasis Telecommunication Systems. The thesis is equivalent to 20 weeks of full time studies.

The authors declare that they are the sole authors of this thesis and that they have not used any sources other than those listed in the bibliography and identified as references. They further declare that they have not submitted this thesis at any other institution to obtain a degree.

Contact Information:

Author:
Subhash Chandra Ranga
E-mail: surn18@student.bth.se

University advisor:
Asso.Prof Siamak Khatibi
Department of Technology and Aesthetics(DITE)

Faculty of Engineering
Blekinge Institute of Technology
SE–371 79 Karlskrona, Sweden

Internet : www.bth.se
Phone : +46 455 38 50 00
Fax : +46 455 38 50 57

Abstract

People around the globe are immensely trying to connect using light as carrier due to its low power consumption and high data transfer rates. Sound and microwaves are examples of other carriers that can be used, although they aren't nearly as efficient as light.A method of communicating is using light beneath the surface of the water. As the depth of the water increases, the temperature, pressure, and salinity of the water are changed. The refractive index of water is determined by the combination of all of these variable parameters.

The goal of this thesis is to establish a relationship between changes in water temperature, salinity, and pressure resulting in changes of the refractive Index of the sea water.This thesis will demonstrate an empirical model of travelling the ultraviolet wave under sea water.We are acknowledging all of the properties that are change as the depth of the water is increasing. MATLAB was used to create a simulation of this scenario. Based on previous model of light traveling which covers the wavelengths between 400-700 nm, we have extended the model to ultraviolet range of light (200-400 nm).We design an experimental set up according to sea water parameters and then the experimental results are compared to the simulation results.The comparison shows the validity of our extension model.

Keywords: Optical Communication, Underwater communication Underwater communication Optical communication, Underwater communication Acoustic communication, Underwater communication Microwave communication, Visible Light Communication, Refractive Index.

Acknowledgments

Writing a scientific thesis is hard work and will not be possible without guidance and support from many people.

First, I would like to thank my thesis advisor Siamak Khatibi, for his guidance with every step of this thesis. Without him this thesis wouldn't see the light of the day.

I would like to extend my gratitude to my family, R.Madhu Sudhana Rao, R.Bala Krishnaveni and R.Akhil Chandra, who are the reason for every thing that I am today. I would also like to take this opportunity to appreciate my future partner Durga Alekhya, for her patience and her never ending support during this thesis. Last but not least, I would like to thanks my friends and well-wisher's.

Contents

Abstract iii

Acknowledgments v

1 Conceptual Background 1
- 1.1 Evolution of light communication . . . 1
  - 1.1.1 UV Spectrum . . . 2
- 1.2 Underwater Communication . . . 2
  - 1.2.1 Underwater Acoustic Communication . . . 3
  - 1.2.2 Underwater Microwave Communication . . . 4
  - 1.2.3 Underwater optical communication . . . 4
- 1.3 Characteristics of water . . . 4
  - 1.3.1 Refractive index . . . 4
  - 1.3.2 Underwater Pressure and Density . . . 5
  - 1.3.3 Underwater Temperature . . . 6
  - 1.3.4 Underwater Salinity . . . 6
- 1.4 Changes in Underwater with Depth . . . 7
  - 1.4.1 Thermocline . . . 7
  - 1.4.2 Pycnocline . . . 7
  - 1.4.3 Halocline . . . 8

2 Introduction to thesis 9
- 2.1 Motivation . . . 9
- 2.2 Aim and Objectives . . . 9
  - 2.2.1 Aim . . . 9
  - 2.2.2 Objectives . . . 9
- 2.3 Research Questions . . . 9
- 2.4 Outline of thesis . . . 10
- 2.5 Related work . . . 10

3 Research Method 13
- 3.1 Literature Review . . . 13
  - 3.1.1 Search Strategy . . . 13
  - 3.1.2 Inclusive and Exclusive Criteria . . . 13
  - 3.1.3 Data Extraction . . . 14
- 3.2 Simulation . . . 16
- 3.3 Experimentation . . . 18
  - 3.3.1 Apparatus . . . 18

3.3.2 Experiment procedure 19
3.3.3 Calibration of image 21
3.3.4 Derivation for shift distance 23

4 Results and discussions **25**
4.1 Results 25
4.1.1 Experiments conducted 27
4.2 Discussions 28

5 Conclusions and Future Work **31**
5.1 Conclusion 31
5.2 Future work 31

References **33**

List of Figures

1.1 EM Spectrum [1] 1
1.2 Different carriers of Underwater communication[2] 3
1.3 Refraction of Light 5
1.4 Snell's law 5
1.5 Changes in depth 7

3.1 Flow chart 15
3.2 Point cloud with Refractive index as intensity 16
3.3 CCD Camera[3] 18
3.4 Light Generator[4] 18
3.5 Side and Top views of Experimental setup 19
3.6 HCImageLive 20
3.7 Checker board 21
3.8 Horizontal values on black and white boxes on checkerboard 21
3.9 Vertical values on black and white boxes on checkerboard 22
3.10 Background 23
3.11 Empty container and Container with water 23
3.12 Shift distance from snells law 24

4.1 RI vs 400nm $< \lambda <$ 600nm 26
4.2 RI vs 350nm $< \lambda <$ 400nm and 200nm $< \lambda <$ 400nm 26
4.3 Change in Refractive index 28

List of Abbreviations

VLC	Visible Light Communication
UV	Ultraviolet
UWSNs	Underwater Sensor Networks
ROVs	Remotely Operated Vehicles
AUVs	Autonomous Underwater Vehicles
UWUC	Underwater Acoustic Communication
QAM	Quadrature Amplitude Modulation
SNR	Signal-to-Noise Ratio
UWMC	Underwater Microwave Communication
UWOC	Underwater Optical Communication
RI	Refractive Index
NOS	National Ocean Service
NOAA	National Oceanic and Atmospheric Administration
FOV	Field Of View
CCD	Charged Coupled Device
PSD	Power Spectral Density

Chapter 1

Conceptual Background

1.1 Evolution of light communication

The entire world is focused on ensuring a more prosperous future for all human beings. A revolutionary upgrade is needed in the field of communication, which is one of the most interesting fields in the world right now. For communication purposes, radio waves and microwaves from the electromagnetic spectrum are now being used to their fullest extent possible. The bandwidth and frequencies of radio waves and microwaves are completely consumed by the transmission of information and data. The entire planet is already on the hunt for new bandwidth and frequencies, such as millimeter waves, sound, and light, to use as carriers for information transmission. Despite the fact that studies on the use of light communication began decades ago, the field of light communication is flourishing. It has been demonstrated that, among all the waves in the electromagnetic spectrum, using the light spectrum for communication has the greatest potential benefit[2]. Aspects such as high data rates, wide bandwidth, and high security are some of the important benefits that can be obtained when using light as a communication carrier. Light is also a cost-effective, low-maintenance, and energy-efficient carrier for communication.

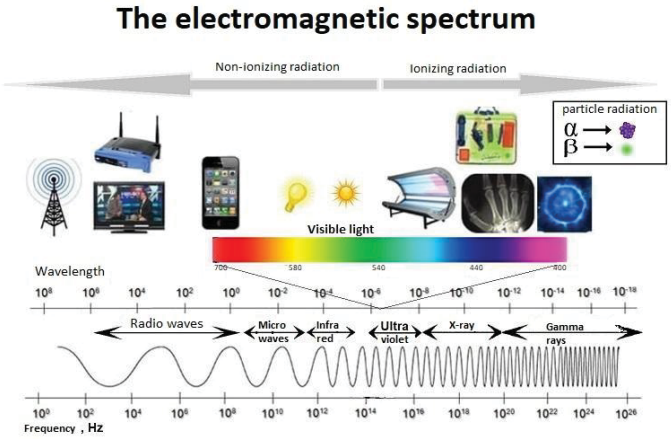

Figure 1.1: EM Spectrum [1]

Several industries are considering using visible light communication (VLC) for the majority of their future projects in the current digital world. Light Fidelity (LIFI) is one of the most promising projects in the VLC. Light can also be used in a variety of mediums with high data rates, such as optical fiber. The authors of these

papers[2] and[5] were successful in demonstrating VLC underwater at a high data rate and over a long distance.

1.1.1 UV Spectrum

We investigate UV penetration depths in our thesis. Ultraviolet (UV) radiation falls within the electromagnetic spectrum and has wavelengths that range from 10 nanometers (about 30 PHz) to 400 nanometers (750 THz), which is shorter than visible light but longer than X-rays[6]. Roughly 10% of the electromagnetic energy produced by the sun comes from UV radiation, and it is present in sunlight. It is created by specific lighting fixtures such as mercury-vapor, tanning, and black lights. UV long-wavelength radiation, which does not ionize atoms, is able to initiate chemical reactions and cause things to fluoresce or glow. Compared to more fundamental heat effects, UV causes many chemical and biological outcomes, and its interactions with organic molecules provide many practical applications.

There are three kinds of UV radiation: long wave, medium wave, and short wave. UVA, the longest wavelength (315–400 nm), is able to penetrate the deepest and is responsible for upwards of 95% of the UV light that passes through the Earth's atmosphere[7]. Radiation of this type promotes skin aging since it penetrates the skin layers deeply (through to the dermis layer). UV radiation may produce skin tanning immediately, and studies have indicated that they are connected to cancer. Unlike the other rays, UVA rays permeate glass and clouds, which causes injury on days with gloomy skies or through your windshield.

The second shortest wavelength, UVB(280nm–315nm), is the major cause of sunburn[7]. The ozone layer largely soaks it up, but some still slips through (about 5 percent gets through overall). You'll burn your skin in as little as 15 minutes with exposure to the sun's rays. Depending on the time of day and season, UVB rays might be more or less intense. UVB rays have a significant correlation with skin cancer. Long-term exposure to UVB radiation can lead to premature aging of the skin.

The 100nm–280nm wavelength is the shortest of the three UV spectrums[8]. UV radiation is more damaging when the wavelength is shorter. Nevertheless, since it is incapable of penetrating the earth's atmosphere, we are in luck. But because the natural UV radiation of the sun cannot pass through skin, the threat is minimal to the average individual. They don't naturally enter the atmosphere of the planet at all. The ozone layer totally absorbs UVC.

The light generator we utilized for this thesis has a maximum range of around $200nm$ to $1200nm$. To carry out our simulation, we put a filter on the camera that blocks all wavelengths except UV-A.

1.2 Underwater Communication

Water is one of the most vital elements in the natural world. It is estimated that water covers around 70% of the earth's surface. Scientists believe that the seas all over the world are responsible for the majority of the changes that occur on Earth.

Researchers have been attempting to model the variations in the behavior of water. Several variables, such as salinity, pressure, and temperature, make water a challenging subject to represent or simulate in computer simulations.

The researchers developed a number of models that provide insight into the link between water salinity, temperature change, and pressure change. These data are essential for the development of better sensors and hence for improved communication. A range of underwater technical activities for real-time monitoring and data transmission, such as Underwater Sensor Networks (UWSNs), Remotely Operated Vehicles (ROVs), and Autonomous Underwater Vehicles (AUVs), are being developed. Because of these activities, it is necessary to have effective systems and procedures. It is also possible for the military to utilize underwater communication to communicate with submarines while on the sea bed, which is referred to as submarine communication. The refractive index of seawater is a function of wavelength (nm), salinity (‰), temperature ($^{\circ}C$), and pressure ($kg/cm2$).To be able to mimic the variations in refractive index behavior, we must first conduct some investigation further into properties of water.

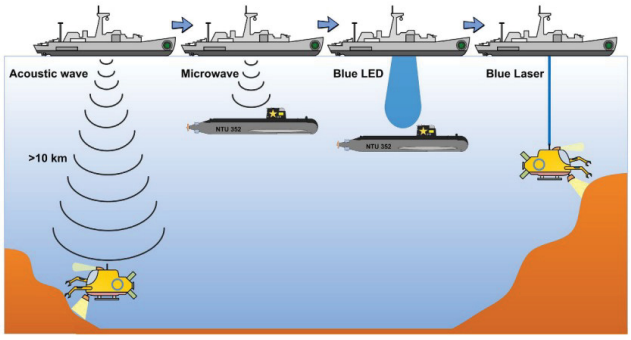

Figure 1.2: Different carriers of Underwater communication[2]

1.2.1 Underwater Acoustic Communication

Underwater Acoustic Communication (UWAC) is a technology for underwater communication that involves use of sound as a means of transmission. The UWAC is a system that has the ability to broadcast signals to a reasonable depth. UWAC systems with 64 quadrature amplitude modulation (QAM) data and 32KHZ bandwidth were proven by Song et al[2]. In a saltwater environment more than 100 meters deep, while Ochi et al. suggested utilizing 32-QAM to create systems with 125 KBPS speeds and low symbol error rates[2]. As a result of these trials, we can observe that the UWAC system is capable of transmitting to greater depths, although the data transfer speed is only 60 KBPS or 12 KBPS (very low). This is due to the fact that the data has a long propagation delay and has a low signal-to-noise ratio (SNR) when compared to the background noise from the water. UWAC systems work best with less distracting backdrops and lighter streaming content. These shortcomings

contribute to the low reliability of UWAC systems.

1.2.2 Underwater Microwave Communication

The Underwater Microwave Communication (UWMC) is the system which had a particular problem. Uribez et al. proposed a UWMC system with an enhanced transmission capacity of 10MBPS per 100m for underwater communication[9]. Due to high attenuation of the microwave, the UWMC system has limited transmission distance i.e. at higher frequencies the UWMC system can provide more bandwidth than the UWAC system. To achieve this bandwidth the power required is about tens of kilowatts which makes UWMC unreliable.

1.2.3 Underwater optical communication

In 2015,[2]demonstrated an LED based single input multi output model. Underwater Optical Communication (UWOC) system that enabled an effective transmission distance over 60 meters. there are several experiments proving its speed. So far it is proved that transmission rates of the underwater optical communication system are high up to 4.3GBPS and 10.2m of distance, When a sub-carrier levelling technique is used on a blue laser diode. The blue color from the sunlight travels up 200 meters of distance. So, if the research on UWOC increases, then the chances of building a better underwater wireless system are more. The problems in UWAC and UWMC can be resolved by using UWOC because the light does not attenuate heavily and is not affected by background noises.

1.3 Characteristics of water

The change in one characteristics of water result in change of another factor. These characteristics of water are completely dependent on each other.

1.3.1 Refractive index

The movement of the light is based on one main feature called refractive index(RI). When the light is travelling from air into water, part of light is reflected and part of it is refracted. Refractive index is defined as the measure of bending of light when it passes from one medium to another. When it come to water the light is affected by temperature, salinity and pressure at respective depth.

Refractive index can be calculated by Snell‘s law.

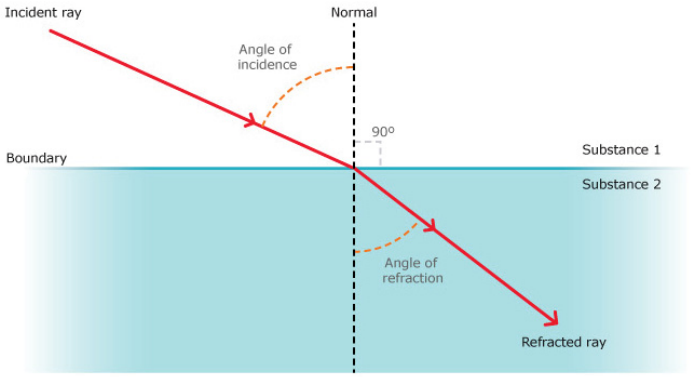

Figure 1.3: Refraction of Light

$$\frac{\sin\theta_1}{\sin\theta_2} = \frac{n_2}{n_1}$$

Figure 1.4: Snell's law

where, n_1 is incident index, $\sin\theta_1$ is incident angle, n_2 is refracted index, $\sin\theta_2$ is refracted angle.

When the refractive index is more, then the velocity of the light is low and vice versa. So, if the refractive index is more than the propagation of light decreases. In this thesis, we have considered the optical refractive index with respect to air. The refractive index of water depends upon temperature, pressure, and salinity.

1.3.2 Underwater Pressure and Density

The pressure and density has an integral relationship. The density of a liquid, soild or gas is the same, which is mass per unit volume. We know that the pressure is defined as force(F) per unit area(A). But when comes to liquids the pressure defined as below [10],

$$P = r * g * h$$

where r is density of liquid, g is acceleration due to gravity and h is height (or) depth. The above formulae is a function of density, acceleration and height because of the disordered motion of the liquid molecules that is why, in this thesis we consider pressure as a variable parameter over density. Pressure is directly proportional to density. If density increases pressure also increases and vise-versa.
The pressure of the underwater is more when compared to the pressure on surface of water. The pressure increases with the depth due the weight exerted by above layers. National Ocean Service(NOS) According to research work by National Ocean Service in National Oceanic and Atmospheric Administration, the pressure of water increases to 1atm for every 10.03m[11]. We consider the above research value in our

thesis for modeling the pressure component.

1.3.3 Underwater Temperature

In general, we know that the temperature of ocean or sea water ranges from -2°C to 40°C[12]. These temperatures are observed when we consider all the water bodies present between north pole and south pole.

In this thesis we consider a balanced temperatures range from 10°C – 30°C. The temperature of water varies with depth. Most of the oceans surface water is has more rapid temperature changes due to sunlight and movement of water.

The surface water sinks towards bottom if it gets colder due to cold weather. The reason why the surface water sinks is because the cold water is denser than the warm water. When the water gets cold the H_2O molecules are tightly packed resulting in increase in density. Since the density increases, they will sink towards bottom. Hence, the colder the water the more it sinks. So, the temperature will decrease with increase in depth due to the increase in density.When the density of sea water is 1.0240 g/cm^3 then the temperature will be 20 °C at 0 °C the density is $1.0273 g/cm^3$ [13].

When compared with salinity changes, the temperature changes will affect the density more. While simulation or experimenting, we must control the temperature more accurately and take good care in maintaining them, so that we get better values of refractive index.

1.3.4 Underwater Salinity

Salinity of ocean water is the measurement of salt present in it. Oceanographers measure the salinity in parts per thousand (ppt). The salinity of water ranges 28 to 40 ppt. The seawater ranges from salinity ranges between 33 to 37 ppt. The salinity of sea water decreases from 3 ppt at the surface to 35 ppt in the deep water. So, in this thesis we will consider the salinity from a ranger of 35 to 36 ppt[14].

Salinity also affects the temperature of seawater. The freezing point of fresh water is 0°C, the freezing point of sea water is -2 °C. Salinity is one of the reasons for maintaining the deep-water temperature constant. Since the change in salinity is low, the change in water density is also low with increasing depth, so does the temperature change.

1.4 Changes in Underwater with Depth

When the depth of the water bodies increases the characteristics of water also changes[?]. These changes are are denoted by certain names when certain characteristics changes.

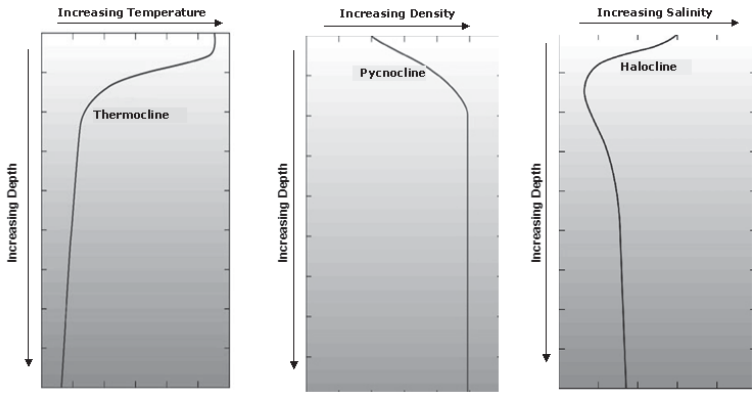

Figure 1.5: Changes in depth

1.4.1 Thermocline

A thermocline is a zone of rapid temperature change that exists in water or air. Because water is not a perfect medium for transmitting light, virtually all sunlight is absorbed in the first few centimeters of the surface layer, resulting in the water heating up. The first few hundred feet of the water's surface layer are well mixed, with the water's temperature more or less consistent. The temperature of the water becomes significantly cooler—potentially dropping by as much as 20 $^{\circ}C$ with an additional 150 meters (500 feet) of depth[15]. The thermocline, or transition zone, is a region of high temperature variability. At the level of the thermocline, temperature starts to decrease, although it does so gradually. Nearly all of the water in the Earth's sea is located below the thermocline. There are several strata of similar density within this deep ocean, which are not combined well.

1.4.2 Pycnocline

It is a fast density gradient in water that occurs when the density of the water changes between the surface layer of water and bottom layer of water. When it comes to freshwater environments, temperature and salinity are the primary factors that influence density change, whereas temperature and salinity may both play a role in changing density when it comes to seawater settings.

1.4.3 Halocline

A halocline is a vertical density gradient that contains a salt-enriched layer at the bottom. Because the salinity of saltwater has an effect on its density, it is possible that it is involved in the process of vertical stratification. Because low-salinity water has a lower density than high-salinity water, it can be found on top of high-salinity water. When it comes to the effects of vertical blending, the results of the density gradient have a significant impact. A deep salt gradient will be difficult to blend, whereas a shallow salt gradient will be simple to blend. Temperature alone does not rule in some sub-Arctic North Pacific waters due to the influence of temperature on density, which is a result of the influence of temperature on density.

Chapter 2

Introduction to thesis

2.1 Motivation

We are fascinated by the concept of a VLC system, which is the primary reason for our thesis. The VLC is the communication method of the future, and it is the most efficient and effective means of doing so. Currently, researchers are studying the use of light underwater. This novel concept for establishing under water light communication inspired us to work on this thesis. To establish underwater optical communication, refractive index is one of the most important properties. In this thesis, we explore the effects of refractive index changes on MATLAB[16] through simulation. We created a real-world environment to test how U.V light penetrates water and also verified our simulation.

2.2 Aim and Objectives

2.2.1 Aim

Aim of this thesis is to replicate the changes of sea water with depth. Since the temperature, salinity and pressure of the water varies with depth very rapidly due to several parameter's .

2.2.2 Objectives

In this thesis we try and simulate a variable environment and model the refractive index. Later we create an real life environment in lab and test the penetration of U.V rays into sea water and compare refractive index values generated with simulation and compare the results.

2.3 Research Questions

RQ1 What parameter's have an impact on the UV region's implementation of underwater communication?

RQ2 How do these parameter's impact the value of the Refractive Index as the depth increases?

RQ3 Determine whether the empirical formula used to calculate the refractive index in the ultraviolet region is accurate or not?

RQ4 How precise are the simulated values in comparison to the experimental ones?

2.4 Outline of thesis

There are four chapters in this thesis. The first chapter of the thesis is about introduction to the underwater communication and light communication. Then we wrote about all possible ways for underwater communication, characteristics of water. We wrote motivation, aim and objective end research questions for this thesis. In second chapter research method, where we wrote about the research method of the thesis, there we discussed about how we gathered the required material for this thesis, simulation, and the experiment. In chapter 3 results and discussion, be sure the results obtained from simulation and the results obtained from experiment and see how bad it is or accurate are the simulated results to experimental results. We also answered all the research questions. a last chapter conclusion and future work, we wrote the conclusion English problems raised in this thesis in the research gap as future work for this thesis.

2.5 Related work

Several different types of methods have been used to find out the feasibility of light penetration under water, The detection of UV penetration in nearshore tropical waters was measured using a easily deploy-able polymer screen by Esther. M. Fleishman. In[17], he used chemical film made up of O-Nitrobenzaldehyde. This chemical polymer film turns into O-nitrobenzoic acid in presence of UV light. Radiation at the surface varies from 5 μmol qunta $s^{-1}m^{-2}$ at the surface to 0.005 at 25m. In this paper a diurnal observations of UV radiation at 1 meter showed a curve comparable to surface plot a synthetically active radiation with a peak of around 1200 hours.

A single mode-laser diode operating inside a Fraunhofer line in coastal water is studied. Numerically in this paper to determine the predicted improvements in an underwater optical system. The performance of silicone PIN direct-detection in the euphotic zone is investigated. In clear sky condition, the solar irradiance is assumed using a lithium niobate interference with various field of view(FOV) properties.

In [18] research they placed an optical filter in front of a receiver, the Power Spectral Density (PSD) of the solar background and the range of transmitted wavelength is treated as noise. Based on standard solar irradians data in parameters of silicone PIN direct-detection receiver, the SNR and FOV of the system is analyzed.

The above two methods does not give us any model considering all the changes in underwater parameters. Later on several instruments are designed to calculate the salinity, temperature and depth of the ocean. The techniques used are proposed in [17].

The research done by Xiaohong QUAN and Edward,to determine an empirical equation for the index of refraction based on changes in temperature, salinity and wavelength[19]. MC.Neil is another author used another empirical formula where it has pressure changes[20]. The paper by Xiaohong has empirical formula at atmospheric pressure.

Both of these authors wrote the empirical formulae from one common research. That research was done by W.austin and George. In [21] paper they tabulated a huge data. Basically, the paper is a review of all the methods during that time and additionally some of advanced changes have been mentioned. In order to get the exact changes in underwater, they considered all of the affecting factors and also their sub factors. This paper and several insitu [22] are also base to my thesis.

A 450nm blue-laser diode modulated with pre-leveled 16-quadrater amplitude modulation(QAM) orthogonal frequency division multiplexing data has been used to achieve it's measurement of transmission capacity. This successfully enabled high speed underwater optical communication over long distances.[2]

Chapter 3

Research Method

The whole thesis was carried out as below:

- Literature Review.
- Simulation.
- Experimentation.
- Documentation.

3.1 Literature Review

IEEE Xplore Digital library and Springe are the data bases used to find most of the papers for this thesis. Since the research towards the underwater optical communication is very less in the aspect that we need, we used some scientific webpages and research papers have been ordered through BTH library are used. To find the papers that answer the question in this thesis we created a Boolean search like "Underwater communication" or "Refractive index of sea water". All the papers that are shown in results of the Boolean search are later selected according to the inclusive and exclusive criteria.

3.1.1 Search Strategy

As a result of string underwater communication, 63 papers have been filtered and selected. Based on paper title 30 papers were picked, while the remaining 33 papers are eliminated from considerations.
Some of old incite measurements and early access papers were opted to leave due to lack of better information. Among the 30 selected papers, only 16 papers were selected after going through the abstracts and relevant topics.

3.1.2 Inclusive and Exclusive Criteria

Inclusive criteria

- Research papers with clear aim.

- Research papers that answer out research questions.
- Research papers having in-site measurement.
- Research papers that are available with full text.

Exclusive criteria

- Research papers that do not address our research topics.
- Research papers that are not in English.
- Research papers that have same or similar topics are eliminated to avoid duplication.

3.1.3 Data Extraction

The papers are divided into 3 types based on the research questions.
The first type of the papers are the papers that discuss about the requirements of RQ1. These papers don't have any empirical formulae or table data to follow.
The second type of the papers are the papers that have the tables and in-site measurements. They have the table and help to answer RQ2.
The third type of the papers are the papers that help in selecting the values for simulation and experimentation. Both second and third type of papers are used to answer RQ3 and RQ4.

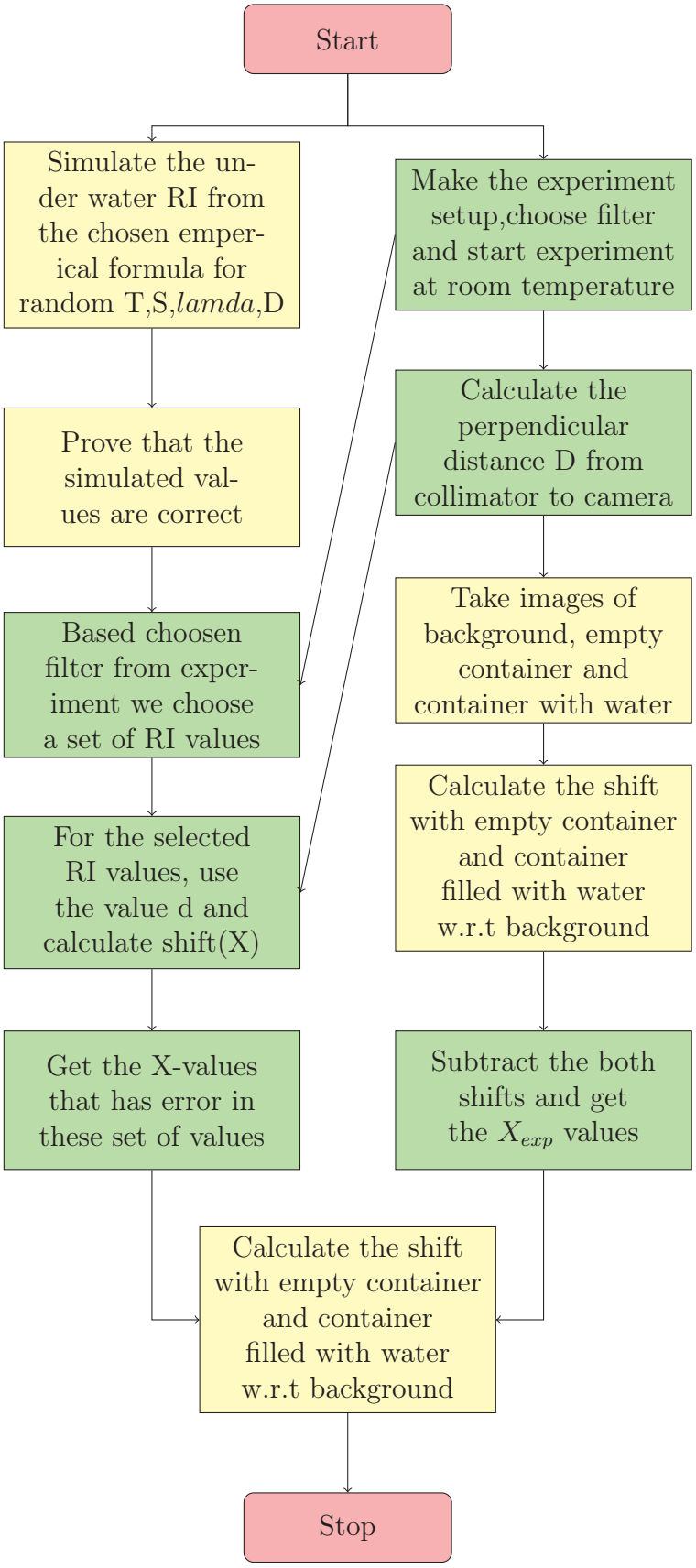

Figure 3.1: Flow chart

3.2 Simulation

For the simulation, we have generated random variables of temperature, salinity, lambda and depth. To calculate the refractive index values, we created a function. The Input to this function is (T,S,λ,depth)=RI, the temperature salinity, λ and depth are picked randomly. This will generate some random refractive index values. We generated it for 10000 × 10000 values of refractive index in MATLAB, as shown in the figure 3.2. If you want a certain set of values or for certain environment like, at T=24° λ=200-400, S=34 to 37 and depth=90m to 100m, we will build this above environment by selecting these values with "AND" condition and collect these refractive index values and then use it to find the shift through equation.

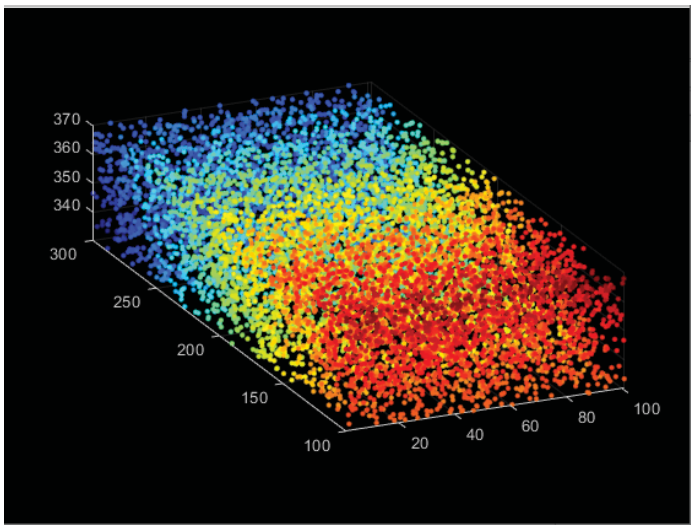

Figure 3.2: Point cloud with Refractive index as intensity

In the paper [19] empirical equation for the index of refraction of seawater written by Xiahong Quan abd Edward S Fry derived an expression to the refractive index as a function of temperature, salinity and wavelength at atmospheric pressure as shown below

$$n(S,T,\lambda) = n_0 + (n_1 + n_2T + n_3T^2)S + n_4T^2 + n_5 + n_6S + n_7T + \frac{n_8}{\lambda^2} + \frac{n_9}{\lambda^3} \quad (3.1)$$

where $n_0 = 1.31405$, $n_1 = 1.779 \times 10^{-4}$, $n_2 = -1.05 \times 10^{-6}$, $n_3 = 1.6 \times 10^{-8}$,$n_4 = -2.02 \times 10^{-6}$,$n_5 = 15.868$,$n_6 = 0.01155$,$n_7 = -0.00423$,$n_8 = -4382$and $n_9 = 1.1455 \times 10^6$ are constants [19].

At first, we built the function with the above expression in matlab end simulated. Since the expression is built with the constant there were some abnormal refractive index values generated. This expression is also not depended upon the pressure which is also one of the reasons for not choosing it. The pressure variation is also one of the most important parameter to be considered when we are dealing with water at increasing depth. In the same paper authors mentioned the origin of the formula[20].

We started working on that empirical formula. The empirical formula that is generated by Gomer T Mcniel in "Material fundamentals of underwater systems" given by Roswell W Austin and George halter in their "inside of refraction of seawater" paper[21].
T Mc Neil loaded the values in a magnetic computer and trained the data to get the following empirical equation for refractive index.

$$n = 1.3247 + 3.3 * 10^3\lambda^{-2} - 3.2 * 10^7\lambda^{-6} - 2.5 * 10^{-6}T^2 + (5 - 2 * 10^2T) \\ (4 * 10^{-5}S) + (1.45 * 10^{-5}P) - (1.021 - 6 * 10^4S)(1 - 4.510^{-3}T) \quad (3.2)$$

Where, n = refractive index
λ = wavelength of light in nm
T = temperature of water in Celsius
S= salinity of water in KG per sqcm
P= pressure of water in KG per sqcm

Since the simulation we want to do is the change in refractive index with increase in depth. As the depth increases the pressure increases because the density changes with increasing depth.
So here the pressure will be per-calculated and will be assigned to formula directly. There is given in the paper that[21]

$$P = (p_0 + p)0.05 * Z$$

p_0 = water density at surface.
p= water density at depth Z.

For the studies of the upper mixed larger of the ocean, the pressure variations are small and is given by P= 0.00000137Z kg/cm^2

If the depth is greater than 100m then we have to follow the pressure value given by Mc Neil, P=0.104Z kg/cm^2[20].

In matlab, the function was created with underwater conditions like temperature, 0 $°C$ < T < 30$°C$, salinity 33‰ < S < 37‰.

The generated refractive index function is then simulated for a random value within these boundary conditions of temperature, salinity for different λ sets.

All the papers so far proposed the empirical formula only for λ range between 400nm to 700nm. So, we check whether this empirical formula can be used for U.V region between 200nm to 400nm. We generated graphs for the change in refractive index values in different ranges of Lambda. We choose the below three ranges randomly,
1. 350 $nm < \lambda <$ 400nm

2. 200 $nm < \lambda < 400nm$
3. 400 $nm < \lambda < 600nm$

The generated graphs are then compared to see whether the refractive index values for empirical formula is accurate or not.

3.3 Experimentation

The aim of this experiment is to find out whether the generated refractive index values for wavelengths in UV range are accurate or not. The simulated results that we got might have an error. So in order to find out how much error is in the simulated values,experiments are conducted and values are tabulated.The experiments are conducted in a perfectly aligned and isolated environment.

3.3.1 Apparatus

The main components of the experiment are Hamamatsu CCD camera and Hamamatsu light generator.

Figure 3.3: CCD Camera[3]

Figure 3.4: Light Generator[4]

The light generator is a lamp based light generator. The light generator can generate a light from 200nm to 1600nm wavelength. Since the entire U.V range which is 200nm to 400nm which is harmful.The whole set up is enclosed in the chamber. The walls of the chamber are made of UV absorbers. This chamber avoids any UV to pass out from the chamber and helps to be safe from UV radiation.

3.3.2 Experiment procedure

The camera is set perfectly in alignment to the light source. The light source generates a beam of light. This beam of light is converted into a thin collimated beam using collimator. The collimator gather all the beam of light originating from the light generator and collimates it into a narrow light.

The camera we used is C800-30 employees on ultra-high sensitivity back thinned CCD sensor which appears in extremely high quantum efficiency in a wide range of UV, VOS and nearby wavelength. This camera has high UV sensitivity from 120nm.

Since the output from the collimator is 200nm to 1600nm but our region of interest is non-visible light region which is 200nm to 400nm. To restrict the band above 400nm, we use a filter in front of the lens of CCD camera. The filter that we chose for our experiment is a bandpass filter. This filter will allow 20nm of band from 370nm-390nm where as the peak of transmission range is 385nm.
The experimental setup is as shown below,

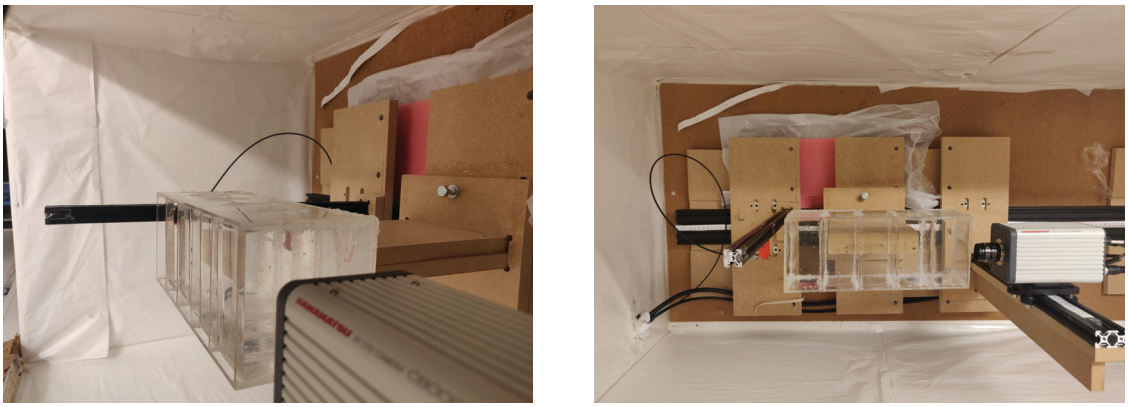

Figure 3.5: Side and Top views of Experimental setup

The generated light is passed through a fiber optic cable into collimator. This collimator is maintained exactly perpendicular to the camera, i.e, the collimator is exactly in 90°C and at the center of the camera lens.
At first, we take an image without placing anything in the background. Then since the container with the water also have refractive index that refracts when take an image , while light is penetrating through it. Each and every time the container is kept at the same position to achieve accurate results. Then the water is placed into

the container. The water we used have different salinity values. As for the salinity values are concern, the procedure of making this sea water is according to this[23], where they explained about recreating a simple ocean water.

The images are captured and processed in separate programs. The images are captured using Hammantsu software called HCImageLive as shown in 3.6. While taking the image, the exposure time is kept constant. The exposure time for all the images is and trigger made is fast frame method used is fast from rate.

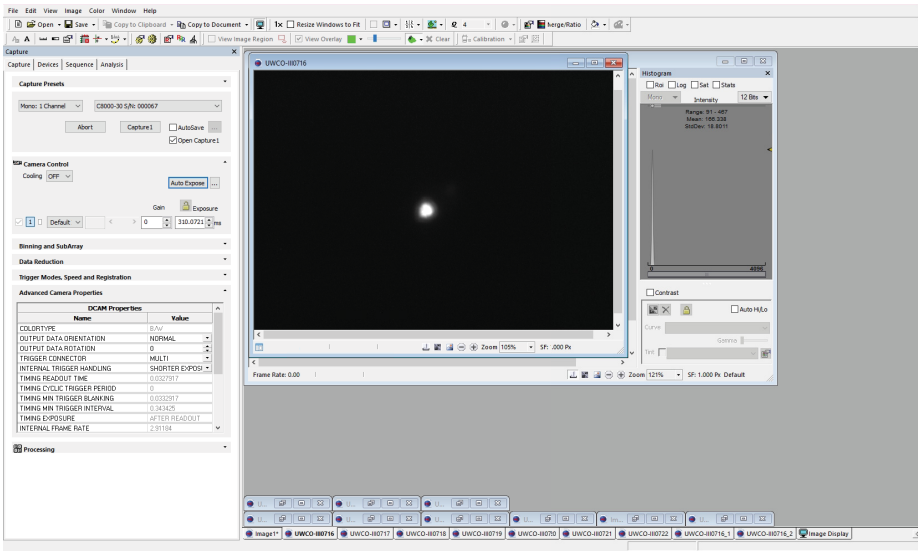

Figure 3.6: HCImageLive

The images are captured and then processed in MATLAB. In MATLAB, we wrote a code that calculate the brightest points of two image and then we calculate the shift by calculating the distance between each of them. The same procedure is repeated on all images from all experiments. Based on this we can find the refractive index. The refractive index depends on that distance derivation is as shown in section 3.4.4.

3.3.3 Calibration of image

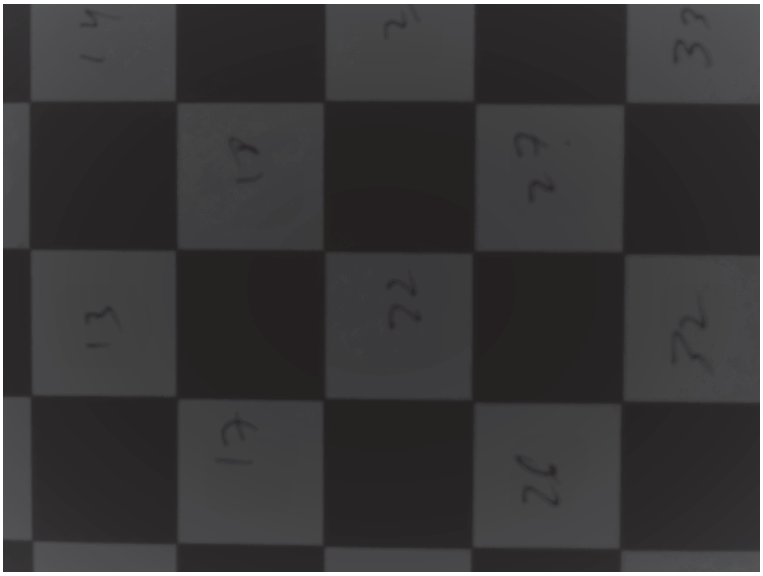

Figure 3.7: Checker board

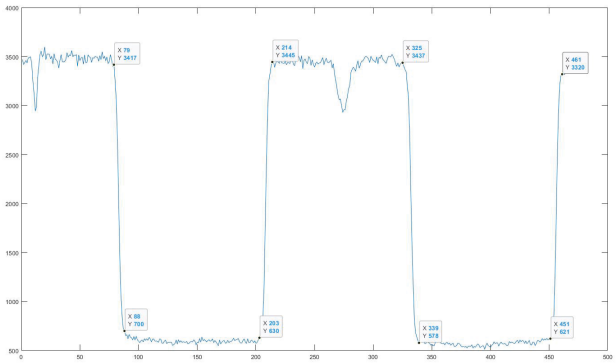

Figure 3.8: Horizontal values on black and white boxes on checkerboard

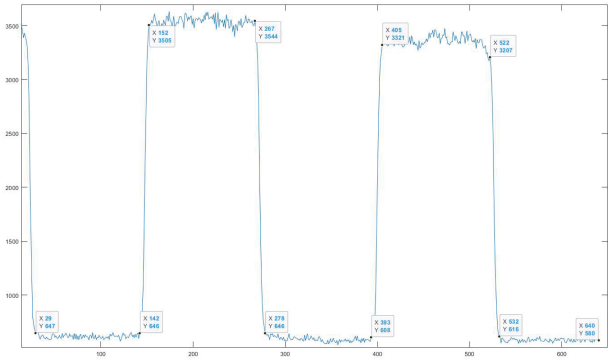

Figure 3.9: Vertical values on black and white boxes on checkerboard

In order to get the distance between two pixels in metric units from the images. The images need to be calibrated. We take the pictures of the checkerboard with 2× 2cm then generate the below graphs.

In this graph we can see the point repeat the values on black and white boxes on checkerboard. By calculating the pixel difference, we get number of pixels for each box. For more accuracy, we repeat this process for vertical image also.From figure 3.8 and 3.9, the average number of pixels is 136. So, according to that distance of the pixels are $\frac{2}{136} = 0.1471mm$. We use this value to calculate distances as in equations 3.3 and 3.4

For the calculation of X_{exp} we'll use the photographs of background, empty container, and container with water. We calculate the shift between empty container with a respective to background eq 3.3 and container filled with water 3.4 with the respective to background.
This shift is calculated by calculating the distance between two points including real world pixel distances as shown below.

$$DstBG_{PC} = \sqrt{(((PCX - BGX) * 0.1471)^2 + ((PCY - BGY) * 0.1471)^2)} \quad (3.3)$$

$$DstBG_{img1} = \sqrt{(((x1 - BGX) * 0.1471)^2 + ((y1 - BGY) * 0.1471)^2)} \quad (3.4)$$

where, PCX and PCY are coordinates of brightest point of an empty container image figure 3.10. BGX and BGY are coordinates of brightest point of background image figure 3.9. x1 and y1 are coordinates of brightest point of container with water image figure 3.10.

Then we subtract the both obtained shifts to get the X_{exp} value. The images of background, empty container, and container with water as shown below in 3.10,3.11,

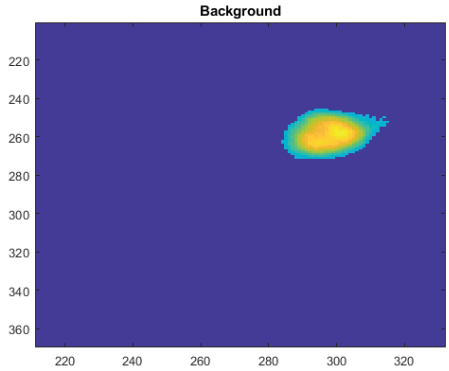

Figure 3.10: Background

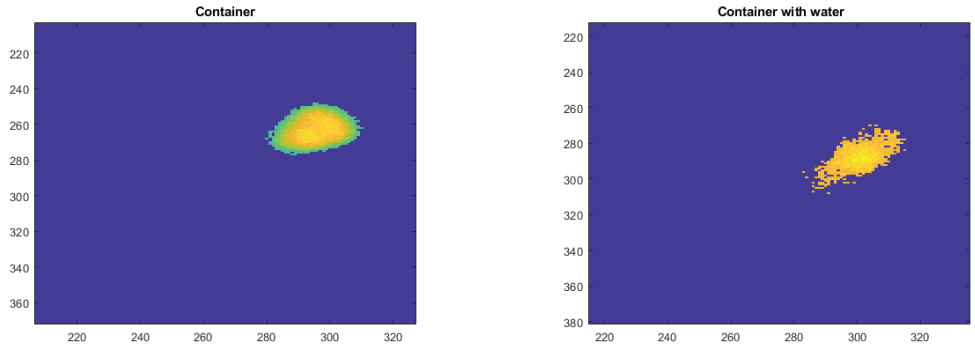

Figure 3.11: Empty container and Container with water

3.3.4 Derivation for shift distance

From Snell's law we know that,

$$\frac{n_2}{n_1} = \frac{sin\theta_1}{sin\theta_2} \tag{3.5}$$

where n_1 = refractive index of air
n_2 = refractive index of water
θ_1 = angle of incidence
θ_2 = angle of refraction

In the experiment, we know that the camera angle is at 90° and n_1 is 1 (refractive index of air)

$$\frac{n_2}{1} = \frac{sin90°}{sin\theta_2}$$

$$sin\theta_2 = \frac{1}{n_2}$$

$$\theta_2 = sin^{-1}\frac{1}{n_2} \tag{3.6}$$

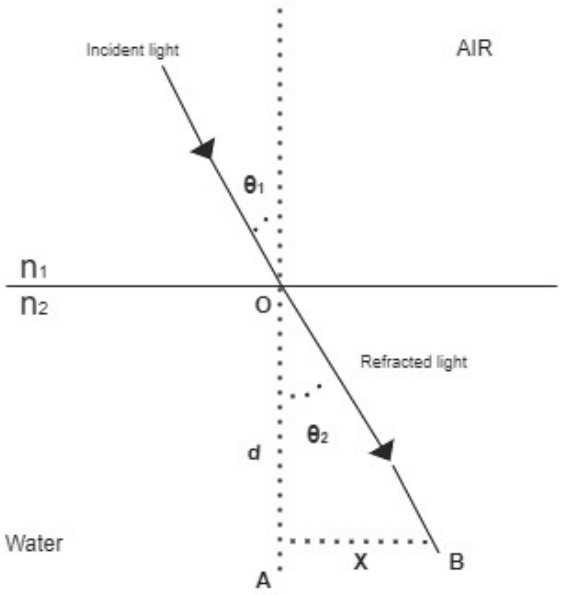

Figure 3.12: Shift distance from snells law

$$\theta_2 \propto \frac{1}{n_2}$$

$$n_2 \propto \frac{1}{\theta_2} \tag{3.7}$$

from the figure 3.12

$$tan\theta_2 = \frac{AB}{OA} = \frac{X}{d}$$

$$X = d * tan\theta_2 \tag{3.8}$$

From 3.8, we know that

$$X \propto \theta_2 \tag{3.9}$$

Susitution 3.9 in 3.7, we get

$$n_2 \propto \frac{1}{\theta_2} \propto \frac{1}{X} \tag{3.10}$$

From the figures we know that the light is going to shift due to presence of water. So, the distance between this is due to change in refractive angle. Then this distance X is compared with the refractive index generated.

Chapter 4

Results and discussions

4.1 Results

From the literature review that we did for this thesis, we found that certain factor like temperature, pressure and salinity will effect refractive index. In [20] at et.al Mc.Neil presented the refractive index of sea water at different depths. In his research he presented an empirical equation to determine the refractive index of sea water and fresh water for practical operational purposes. Mc.Neil determined this empirical equation from the data recorded in research done by Roswell W. Austin and George Halikas. They recorded huge data, based on this data Mc.Neil proposed the empirical equation of refractive index as a function of temperature, salinity, wavelength and pressure at different depths.

The empirical formula is valid for the certain condition of temperatures($0°C < T < 30°C$), salinity ($0‰o < S < 30‰o$) and wavelengths ($400nm < \lambda < 700nm$). In this thesis we consider the values observed by the researchers at National Ocean Service (NOS) in National Oceanic and Atmospheric Administration (NOAA), Optical society (OSA publishers). According to their research, the temperature changes with depth is $10°C < T < 30°C$ [15] and salinity changes with depth is $33‰o < S < 37‰o$.

In the simulation, we considered the above values of temperature, salinity, pressure and wavelengths for different depths. Then we calculate the refractive index values, which are decreasing for $400nm < \lambda < 700nm$. The refractive index value $700nm$ wavelength is 1.3316 and refractive index value $400nm$ wavelength is 1.3748. Clearly we can say that with decreasing wavelength the value of refractive index is high. The velocity of light is low at lower wavelengths since the refractive index values is high. This phenomenon does not effect much for the changes temperature, salinity and depth.

We created graphs to illustrate the change in refractive index values over a variety of λ values. We select randomly three ranges below.In order to compare and judge on continuity we consider lambda that are valid for the eq 3.2 and also the wavelengths of UV region. 1 and 2 are in UV region 3 is in between $400nm < \lambda < 700nm$[20].
1.350nm $< \lambda <$ 400nm
2.200nm $< \lambda <$ 400nm
3.400nm $< \lambda <$ 600nm

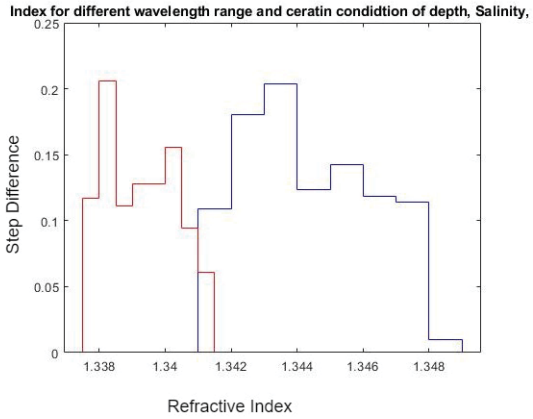

Figure 4.1: RI vs 400nm $< \lambda <$ 600nm

The above graph is generated for the wavelengths ranging from 400nm $< \lambda <$ 600nm.

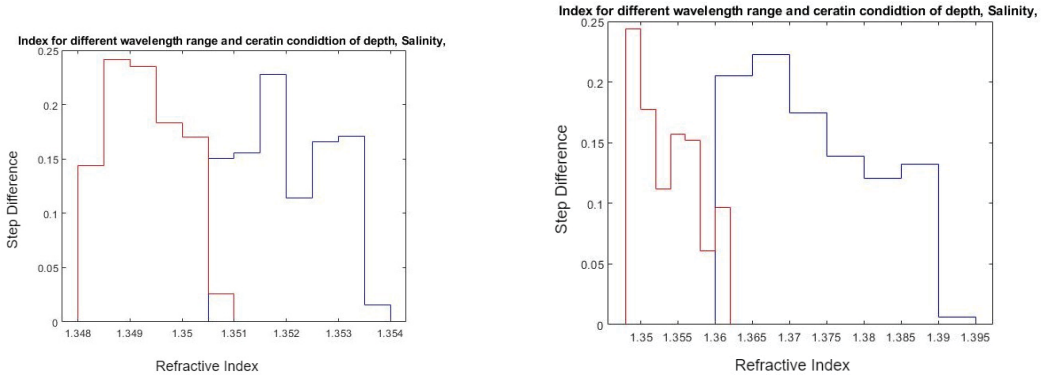

Figure 4.2: RI vs 350nm $< \lambda <$ 400nm and 200nm $< \lambda <$ 400nm

The above figure 4.2, is generated wavelengths ranging from 350nm $< \lambda < 400nm$ and $200nm < \lambda < 400nm$ which are wavelengths of UV range.
It is clear from the patterns in the graphs, the refractive index values generated by empirical formula at wavelengths $200nm < \lambda < 400\ nm$ range follows the same pattern as we generated in figure 4.2. So, we can consider this continuity in the pattern as a proof that the chosen empirical formula is valid for wavelengths $200nm < \lambda < 400nm$ i.e, UV range.

As seen above, similar empirical formulae are now also employed in the ultraviolet area. Thus, we now construct several instances for the purpose of comparing the values obtained by simulations and experiments. In these real-time tests, we utilize a camera to see the shift in the light, but in simulation, we will compute the shift in the picture (X) using the produced RI values. We will compare the shift values of experimented and simulate and then determine the inaccuracy and the simulation's accuracy based on the difference between them.

4.1.1 Experiments conducted

We assumed the five partitions of our container to be 100m deep in all of our trials. Thus, each partition is 20 m deep, and in Experiment Set 4, we will fill in the salinity values at those depths for each partition and measure the difference in that order. To determine the outcome of the experiment, their individual background pictures and exposure times are factored into the final output. All studies utilized a single band-pass filter with a pass-band of 370nm to 390nm.

Experiment No. 1: The first partition of the water container contains 33 percent salty water. The shutter speed of the camera is set at 5.6. 120.76ms is the exposure time. At 24 degrees, the temperature is considered to be at room temperature.

Experiment No. 2: The water container with the first partition filled to 35% with saline water. The shutter speed of the camera is set at 5.6. 120.76ms is the exposure time. At 24 degrees, the temperature is considered to be at room temperature.

Experiment No. 3: Fill a water container with 36 percent saline water in the fifth partition. The shutter speed of the camera is set at 5.6. 512.13ms is the exposure time. At 24 degrees, the temperature is considered to be at room temperature.

Experiment No. 4:
Case 4.1: Fill a water container with 36% saline water in the fifth partition and 35% saline water in the fourth partition.The shutter speed of the camera is set at 5.6. 512.13ms is the exposure time. At 24 degrees, the temperature is considered to be at room temperature.

Case 4.2: Fill a water container with 36% saline water in the fifth partition, 35% saline water in the fourth partition, and 34% saline water in the third partition. The shutter speed of the camera is set at 5.6. 512.13ms is the exposure time. At 24 degrees, the temperature is considered to be at room temperature.

Case 4.3: Fill a water container with 36% saline water in the fifth partition, 35% saline water in the fourth divider, 34% saline water in the third partition, and 33% saline water in the second partition. The shutter speed of the camera is set at 5.6. 512.13ms is the exposure time. At 24 degrees, the temperature is considered to be at room temperature.

Case 4.4: Fill a water container to the brim with 36% saline water in the fifth partition, 35% saline water in the fourth partition, 34% saline water in the third partition, 33% saline water in the second partition, and surface seawater in the first partition. The shutter speed of the camera is set at 5.6. 512.13ms is the exposure time. At 24 degrees, the temperature is considered to be at room temperature.

EXPERIMENT NO	**X**$exp(mm)$	**X**(mm)	**Error**(mm)	**Variance**(mm)
Experiment NO1	1.4906	4.7239	3.2333	$9.8471e^{-06}$
Experiment NO2	0.4161	4.7226	4.3065	$9.0121e^{-06}$
Experiment NO3	0.1135	4.7215	4.6080	$9.0035e^{-06}$
Experiment NO4(Case4.1)	1.2273	4.7218	3.4945	$1.0683e^{-05}$
Experiment NO4(Case4.2)	0.2137	4.7216	4.5079	$1.2502e^{-05}$
Experiment NO4(Case4.3)	1.6049	4.7215	3.1167	$1.4466e^{-05}$
Experiment NO4(Case4.4)	3.1458	4.7216	1.5758	$1.4468e^{-05}$

Table 4.1: Comparison of shift distances in experiment and simulated values

4.2 Discussions

In this section, research questions that are mentioned in research method section are answered.

[RQ1] What parameter's have an impact on the UV region's implementation of underwater communication?

From this thesis literature review, we have found that the parameter's that are effecting the UV penetration is temperature, salinity, pressure and depth.That means the refractive index is function of temperature, salinity, pressure and wavelengths.Salinity is the amount of salt present in 1 liter of water. The temperature, salinity, pressure changes with depth so does the refractive index of water changes.This change in the parameter's leads to change in refractive index.Due to change in refractive index it is hard to penetrate the UV range wavelengths to penetrate.

[RQ2] How do these parameter's impact the value of the Refractive Index as the depth increases?

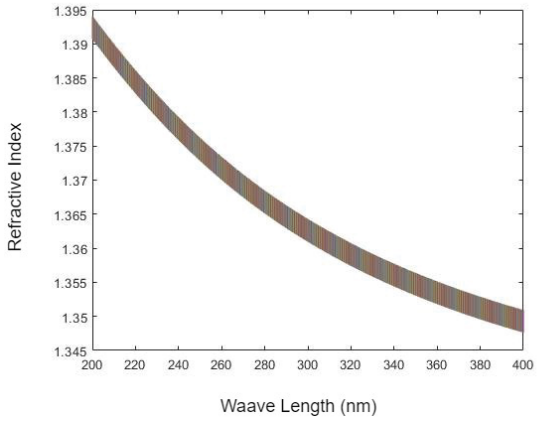

Figure 4.3: Change in Refractive index

From the figure 4.3, we can see that the Refractive index values changes linearly

with the wavelength of the light. In UV region when the values increases from $200nm$ to $400nm$, the values of the refractive refractive index decreases. It is clear from the section 4.1, how the shifting of the light changes within UV region.

It is clear from [20] Table 2 that the pressure increases with depth. The amount of water above increases with increase in depth so do the pressure. From [21] Table A-5, we can see that the refractive index is increasing with increase in pressure.

From [21] Table A-1, at atmospheric pressures with increase in salinity the value of the refractive index is also increasing. But when the salinity is kept constant and the temperatures are increased then the refractive index is decreasing.

[RQ3] Determine whether or not the empirical formula used to calculate the refractive index in the ultraviolet region is accurate ?

We have generated a very big matrix (10000*10000) as shown in fig?? of RI values. Each refractive index values are generated from a random values of temperature, salinity,wavelengths and depths.Among all these values we have collected few sets of data based on its wavelengths to check the continuity in the pattern.According to [20] the empirical formulae eq?? is valid only for $400nm < \lambda < 700nm$.

Before using the empirical formulae in UV region we need to check if the formulae is valid in $200nm < \lambda < 400nm$ or not. So we select the values $350nm < \lambda < 400nm$ and $200nm < \lambda < 400nm$ in UV range $200nm < \lambda < 400nm$. In the results section, we have proved how the values of the chosen empirical formulae is following the pattern for the UV region also. Since the chosen empirical formulae followed the pattern we used it in our experiments.

[RQ4] How precise are the simulated values in comparison to the experimental ones?

We know that the empirical formulae are true in the ultraviolet area. We're now going to construct the experimental setup. We can alter the salinity of water and add varying quantities of salt. For example, if we want a salinity value of 36%, we combine 64 ml water with 36g salt. Now, in accordance with the experiments detailed in the results section, we build an environment and conduct the experimental method. The same image processing is followed for all the experiments. Then we will select the RI values generated from simulation according to the values used in each experiment and calculate the shift distance from them.

In the results, we have shown how much difference the values i.e. errors and their respective variances. We found that The experiment's shift value is decreasing, indicating that the experimental and simulated findings are profoundly in the same order. As the shift values are decreasing with the increase in salinity ,the refractive index of water decreases, eq3.10 .From the literature review we know that refractive index of water decreases with increase in salinity.

Chapter 5

Conclusions and Future Work

5.1 Conclusion

The shifts that are generated from simulation have maintained almost constant variation. But the shifts that are generated from experiment are interestingly increasing with increasing depth i.e, when there is only one partition is filled with different salinity in experiment 1, experiment 2, experiment 3, there is more error. As the salinity of water is increased from 33%o, 35%o, 36%o respectively. The shift value of the experiment is decreasing which means, actually the experiment results and simulated results are following the same order as we found from literature reviews. Since the refractive index of water is increasing with increase in salinity. If the refractive index increases, shift values of experiment or simulation decrease as from eq 3.9.

From the experiment four, we have seen that X_{exp} is increasing with increasing in depth except in case 4. But clearly from eq 3.10, we can say that X_{exp} value is rapidly increasing for rest of the cases(1,2,3). If the refractive index values are decreased the velocity of light is increased that is the chances of penetration are more. The experimented values are following a correct flow but when comparing them with the simulated results, but the error is high. The X values a decreasing when we are moving towards creating a real time scenario. There are between both the shifts are high but if we observe the values of X, they are also following a pattern. For experiment 1, experiment 2 an experiment 3 the X values decreased with increasing salinity. But when the depth is increasing ,the X values from simulation are constant.

5.2 Future work

Due to lack of time and resources, numerous modifications, testing and study have been left for future. the following hypothesis could be tested,

- If we observed from the from table 3.1, we could see that shift difference of simulated and experimented shift value is large. This is due to empirical formula generated at real depths in experiments are done at assumed depths.
- The experiment needs to change do an exact simulating scenario then we can see more accurate results.
- The experiment we have conducted are very less, it could be better if more experiments were conducted by considering real environment like using actual

sea water than a substitute sea water.

- It would be more interesting if one can simulator the temperature changes into experiment.
- Experimenting in a 100m deep tank will also be more interesting because with more depth, pressure can be taken into consideration.
- Finding a better filter with 100% efficiency in transmitting the UV light at different wavelengths will help in finding the penetration at different wavelengths of light.
- Conducting more experiments by changing different band pass filters in UV range.

References

[1] UNIVERSITY OF BERGEN em spectrum. https://www.uib.no/en/hms-portalen/75292/electromagnetic-spectrum. Accessed: 2021-08-23.

[2] Tsai-Chen Wu, Yu-Chieh Chi, Huai-Yung Wang, Cheng-Ting Tsai, and Gong-Ru Lin. Blue laser diode enables underwater communication at 12.4 gbps. *Scientific reports*, 7(1):1–10, 2017.

[3] Hamamatsu. C.c.d camera. https://www.hamamatsu.com/eu/en/product/cameras/ccd-cameras/index.html.

[4] Hamamatsu. Deuterium lamp generator. https://www.hamamatsu.com/eu/en/product/light-and-radiation-sources/lamp/deuterium-lamp/index.html.

[5] Jing Xu, Yuhang Song, Xiangyu Yu, Aobo Lin, Meiwei Kong, Jun Han, and Ning Deng. Underwater wireless transmission of high-speed qam-ofdm signals using a compact red-light laser. *Opt. Express*, 24(8):8097–8109, Apr 2016.

[6] Esther M Fleischmann. The measurement and penetration of ultraviolet radiation into tropical marine water. *Limnology and Oceanography*, 34(8):1623–1629, 1989.

[7] STOUCHLIGHTING. What is the difference between uva uvb uvc?

[8] Wikipedia contributors. Ultraviolet — Wikipedia, the free encyclopedia, 2021. [Online; accessed 12-September-2021].

[9] Carlos Uribe and Walter Grote. Radio communication model for underwater wsn. In *2009 3rd International Conference on New Technologies, Mobility and Security*, pages 1–5. IEEE, 2009.

[10] Robert Tenzer, Pavel Novák, and Vladislav Gladkikh. On the accuracy of the bathymetry-generated gravitational field quantities for a depth-dependent seawater density distribution. *Studia Geophysica et Geodaetica*, 55(4):609–626, 2011.

[11] NOAA. How does pressure change with ocean depth? https://oceanservice.noaa.gov/facts/pressure.html#:~:text=This%20is%20due%20to%20an,pressure%20increases%20by%20one%20atmosphere%20.

[12] Elahe Akbari, Seyed Kazem Alavipanah, Mehrdad Jeihouni, Mohammad Hajeb, Dagmar Haase, and Sadroddin Alavipanah. A review of ocean/sea subsurface water temperature studies from remote sensing and non-remote sensing methods. *Water*, 9(12):936, 2017.

[13] Exploring Our Fluid Earth. Ocean temperature profiles. `http://manoa.hawaii.edu/exploringourfluidearth/physical/density-effects/ocean-temperature-profiles`.

[14] Xiaodong Zhang, Dariusz Stramski, Rick A. Reynolds, and E. Riley Blocker. Light scattering by pure water and seawater: the depolarization ratio and its variation with salinity. *Appl. Opt.*, 58(4):991–1004, Feb 2019.

[15] John Hood. How does temperature affect refraction of water? ee rough draft.

[16] *Matlab version 9.5.0 (R2019b).* Accessed: 2021-08-23.

[17] Giovanni Giuliano, Leslie Laycock, Duncan Rowe, and Anthony E Kelly. Solar rejection in laser based underwater communication systems. *Optics Express*, 25(26):33066–33077, 2017.

[18] Shashank Kumar Singh and Nirbhay Kumar Tagore. Underwater based adhoc networks: A brief survey to its challenges, feasibility and issues. In *2019 2nd International Conference on Signal Processing and Communication (ICSPC)*, pages 20–25. IEEE, 2019.

[19] Xiaohong Quan and Edward S Fry. Empirical equation for the index of refraction of seawater. *Applied optics*, 34(18):3477–3480, 1995.

[20] Gomer T McNeil. Metrical fundamentals of underwater lens system. *Optical Engineering*, 16(2):162128, 1977.

[21] Roswell W Austin and George Halikas. The index of refraction of seawater. 1976.

[22] Junyao Chen, Wenping Guo, Min Xia, Wei Li, and Kecheng Yang. In situ measurement of seawater salinity with an optical refractometer based on total internal reflection method. *Opt. Express*, 26(20):25510–25523, Oct 2018.

[23] E. His, R. Beiras, and M.N.L. Seaman. The assessment of marine pollution - bioassays with bivalve embryos and larvae. volume 37 of *Advances in Marine Biology*, pages 1–178. Academic Press, 1999.

Faculty of Engineering, Blekinge Institute of Technology, 371 79 Karlskrona, Sweden